The Astronomical Journal, 165:127 (11pp), 2023 March https://doi.org/10.3847/1538-3881/acabc0

Optical Spectroscopic Observations of Gamma-Ray Blazar Candidates. XII. Follow-up Observations from SOAR, Blanco, NTT, and OAN-SPM

Abigail García-Pérez[1,2], Harold A. Peña-Herazo[3], Francesco Massaro[2,4,5,6], Vahram Chavushyan[1,7], Raffaele D'abrusco[7], Nicola Masetti[8,9], Marco Landoni[10,11], Fabio La Franca[12], Víctor M. Patiño-Álvarez[1,13], Raúl A. Amaya-Almazán[1], Dan Milisavljevic[14], Alessandro Paggi[2,4,5], Federica Ricci[8,12], Elena Jiménez-Bailón[15], and Howard A. Smith[7]

[1] Instituto Nacional de Astrofísica, Óptica y Electrónica, Luis Enrique Erro 1, Tonantzintla, Puebla 72840, México; abigail.garciapz@gmail.com
[2] Dipartimento di Fisica, Università degli Studi di Torino, via Pietro Giuria 1, I-10125 Torino, Italy
[3] East Asian Observatory, 660 N. A'ohōkū Place, Hilo, HI 96720, USA
[4] Istituto Nazionale di Fisica Nucleare, Sezione di Torino, I-10125 Torino, Italy
[5] INAF-Osservatorio Astrofisico di Torino, via Osservatorio 20, I-10025 Pino Torinese, Italy
[6] Consorzio Interuniversitario per la Fisica Spaziale (CIFS), via Pietro Giuria 1, I-10125, Torino, Italy
[7] Center for Astrophysics | Harvard & Smithsonian, 60 Garden Street, Cambridge, MA 02138, USA
[8] INAF-Osservatorio di Astrofisica e Scienza dello Spazio, via Gobetti 93/3, I-40129 Bologna, Italy
[9] Instituto de Astrofísica, Facultad de Ciencias Exactas, Universidad Andrés Bello, Fernández Concha 700, Las Condes, Santiago RM, Chile
[10] INAF-Osservatorio Astronomico di Cagliari, via della Scienza, 5, Selargius, Cagliari, Italy
[11] INAF-Osservatorio Astronomico di Brera, Via Emilio Bianchi 46, I-23807 Merate, Italy
[12] Dipartimento di Matematica e Fisica, Universitá Roma Tre, via della Vasca Navale 84, I-00146 Roma, Italy
[13] Max-Planck-Institut für Radioastronomie, Auf dem Hügel 69, D-53121 Bonn, Germany
[14] Department of Physics and Astronomy, Purdue University, 525 Northwestern Avenue, West Lafayette, IN 47907, USA
[15] Instituto de Astronomía, Universidad Nacional Autónoma de México, Apdo. Postal 877, Ensenada, 22800 Baja California, México
Received 2022 June 27; revised 2022 October 4; accepted 2022 December 13; published 2023 February 23

Abstract

Roughly one third of the sources in the Fermi-LAT catalogs are listed as unidentified/unassociated γ-ray sources (UGS), i.e., they lack a low-energy counterpart. In addition, there is a growing population of blazars of uncertain type (BCUs). Spectroscopic observations are crucial to confirm the blazar nature of the UGSs candidate counterparts and BCUs. Hence, in 2013 we started an optical spectroscopic campaign to carry out the identifications and classifications. In this paper, as a continuation of the campaign we report the spectra of 39 sources: the sample comprises 37 sources classified as BCUs, one source classified as a BL Lac in the Fourth Source Catalog of the Fermi-LAT (4FGL), and one source classified as UGS. We classify 19 of the sources in the sample as BL Lacs, 13 as blazars with nonnegligible host-galaxy emission, six as Flat Spectrum Radio Quasars, and one as a normal elliptical galaxy. The source listed as BL Lac in the 4FGL seems to be a blazar with nonnegligible host-galaxy emission in our observations, most likely due to an ongoing quiescent state. We classified the UGS source as a BL Lac. Six out of the 39 sources were previously reported in the campaign; in general, both the classifications and redshifts are in agreement, except for one of them with no redshift reported before. Altogether, we provided reliable redshift estimates to 21 out of the 39 sources. Finally, we describe the statistics of the data collected in our campaign so far.

Unified Astronomy Thesaurus concepts: Optical identification (1167); Blazars (164); BL Lacertae objects (158); Flat-spectrum radio quasars (2163)

Supporting material: extended figures

1. Introduction

The Fermi Large Area Telescope (Fermi-LAT) was launched in 2008 to improve our understanding of high-energy emitting sources, their underlying astrophysical mechanisms, and to fulfill the need for a more powerful tool to study them, opening the way for a new era in γ-ray astronomy (Atwood et al. 2009). Thanks to its continuous survey of the sky since its launching, the most recent Fermi-LAT catalog includes more than 5000 sources observed in the 50 MeV–1 TeV energy range. These observations have greatly helped to resolve the γ-ray sky and have enriched multimessenger astronomy, allowing the scientific community to carry out deep studies on different γ-ray sources over the years, from supernova remnants (Acero et al. 2016) to Gamma-ray bursts (Ackermann et al. 2013; Ajello et al. 2019) and active galactic nuclei (Abdo et al. 2010a; Ackermann et al. 2011; Cutini et al. 2014; Ajello et al. 2020), the latter specifically regarding multifrequency analysis of blazars and their spectral energy distributions. For the extragalactic γ-ray sky, in particular for the largest population of associated γ-ray sources: the blazars, their number significantly increased during all these years of Fermi operation. In the first release of the Fermi catalog (1FGL; Abdo et al. 2010a) there were ~570 blazars detected in the MeV–GeV energy range in addition to nearly 100 active galactic nuclei showing similar properties, while we count more than 2200 blazars in the 3rd release of the 10 yr Fermi Source Catalog (4FGL-DR3; Abdollahi et al. 2022) and ~1500 γ-ray sources sharing similar behavior and thus being labeled as blazars of uncertain type (BCUs).

One of the major difficulties that Fermi-LAT still faces in the study of γ-ray sources is to find their low-energy counterparts, since the Fermi-LAT has positional uncertainties of the order of $0^{\circ}.1$. For this reason, it is imperative to develop and apply more precise association methods. From all previous Fermi-LAT catalogs (1FGL, 2FGL, 3FGL, and 4FGL[16] in Abdo et al. 2010b, Nolan et al. 2012, Acero et al. 2015, and Abdollahi et al. 2020, respectively), blazars were found to be the most abundant sources of γ-rays. This fact that has been convenient for source association, especially for the study of unidentified/unassociated γ-ray sources (UGSs; sources that lack a firm association with a low-energy counterpart), which is one of the main goals of Fermi-LAT. It is worth highlighting that the fraction of UGSs remains fairly constant during the releases of all Fermi catalogs. This is mainly due to all multifrequency follow-up campaigns carried out to discover new pulsars and blazars, the two largest population of associated γ-ray sources.

According to the unified model of active galactic nuclei (AGNs), blazars are those AGNs whose jet is closely aligned to our line of sight (Urry & Padovani 1995). They have the largest and most rapid variations (with timescales from years down to hours or even minutes) of all AGNs at all wavelengths; for example, Wagner & Witzel (1995) found variations of minute timescales in the optical band, with amplitudes of up to 20%. Blazars are classified as BL Lacs and Flat-spectrum radio quasars (FSRQs) on the basis of their optical spectra (Stickel et al. 1991; Stocke et al. 1991). BL Lacs are those with featureless optical spectrum or with emission lines with equivalent widths (EWs) of less than 5 Å, while FSRQs show quasar-like spectra with flat radio spectrum and highly polarized emission from radio to optical frequencies (e.g., Healey et al. 2007; Hovatta et al. 2012). Another quantitative difference is the luminosity of the broad-line region measured in Eddington units, with values of $L_{\rm BLR}/L_{\rm Edd} < 5 \times 10^{-4}$ for BL Lacs, which is related to the lower magnetic field strengths and lower accretion rates of BL Lacs with respect to FSRQs (Ghisellini et al. 2011).

About 40% of the blazars in the 4FGL-DR3 are BCUs; these sources have no optical spectroscopic information available to classify them. Since the first release of the Fermi-LAT catalogs, most of the blazars on them are BL Lacs rather than FSRQ; for this reason, we are expecting to discover more BL Lacs among BCUs and UGSs. It is also worth noting that, although the number of radio galaxies on each release is small with respect to the one of blazars, it has increased to 42 in the 4FGL catalog.

One of the methods employed to investigate the low-energy counterpart of UGSs involves the mid-IR WISE colors: in a [3.4]–[4.6]–[12] μm color–color diagram, blazars tend to group in a specific region clearly separated from the other extragalactic sources that are dominated by thermal emission (Massaro et al. 2011; D'Abrusco et al. 2012). With this discovery in mind, the growing population of BCUs, the total amount of UGSs, and the need for confirmation of their nature, we started our spectroscopic campaign to identify and classify potential low-energy counterparts of UGSs and confirm the blazar nature of BCUs. We adopted the same classification labels of the Roma-BZCAT, i.e., BZB for BL Lacs, BZQ for FSRQs, and BZG for those blazars with nonnegligible host-galaxy emission in their optical spectra and spectral energy distributions (Massaro et al. 2012), similar to elliptical galaxies in the optical band. As stated before for FSRQs and BZBs, BZQs are those sources with quasar-like spectra and broad emission lines, and BZBs have typical featureless optical spectra that in rare cases could show weak emission lines of equivalent width lower than 5 Å and/or absorption features due to gas and dust residing in their host galaxies (Stickel et al. 1993). The difference between BZBs and BZGs is that BZBs show strong blue continuum, do not possess Ca II H&K break or the flux densities at higher frequencies than the Ca II H&K break have a similar level or higher than the flux densities at lower frequencies; otherwise, the source is a BZG (Landt et al. 2002).

Throughout our optical spectroscopic campaign, which started in 2013 (Paggi et al. 2014; Landoni et al. 2015b; Massaro et al. 2015; Ricci et al. 2015; Álvarez Crespo et al. 2016a, 2016b; Peña-Herazo et al. 2017; Marchesini et al. 2019; Peña-Herazo et al. 2019; de Menezes et al. 2020; Peña-Herazo et al. 2021a), we have been able to classify 337 sources as BZBs, 51 as BZQs, and 47 as BZGs. We have also provided redshifts (z) for several of them, including 82 of the BZBs that did not possess redshift estimates before. The optical spectroscopic observations analyzed during the campaign have been collected from several telescopes, such as the Víctor Blanco Telescope at Cerro Tololo Inter-American Observatory, Guillermo Haro Astrophysics Observatory, Loiano Cassini Telescope, Magellan Telescopes at Las Campanas Observatory, Mayall 4 m Telescope at Kitt Peak National Observatory (KPNO), Multiple Mirror Telescope, the 2.1 m telescope of the National Astronomical Observatory San Pedro Mártir (OAN-SPM), New Technology Telescope (NTT), Nordic Optical Telescope, Palomar Observatory, Southern Astrophysical Research (SOAR) Telescope, Telescopio Nazionale Galileo, and the William Herschel Telescope. Most of the data employed during the campaign has been acquired from SOAR (133 sources), OAN-SPM (75 sources), KPNO (55 sources), and Víctor Blanco (44 sources).

The spectroscopic identifications of our campaign have been used for other authors to: build the luminosity function of BL Lacs (Ajello et al. 2014), which in turn contributes to better the understanding of the extragalactic γ-ray background (Ajello et al. 2015); select potential targets for the Cherenkov Telescope Array (Massaro et al. 2013b; Arsioli et al. 2015); obtain stringent limits on the dark matter annihilation in subhalos (e.g., Zechlin & Horns 2012; Berlin & Hooper 2014); search for counterparts of new flaring γ-ray sources (Bernieri et al. 2013); test new γ-ray detection algorithms (Campana et al. 2015, 2016); perform population studies on the UGSs (e.g., Acero et al. 2013); and to discover the new subclass of radio weak BL Lacs (e.g., Massaro et al. 2017).

Recent optical spectroscopic campaigns have found that most of the potential low-energy counterparts of UGSs and classified BCUs are identified as BL Lacs (see, e.g., Landoni et al. 2015a; Massaro et al. 2016; Klindt et al. 2017; Marchesi et al. 2018; Desai et al. 2019; Paiano et al. 2019). This has shown that BL Lacs are the most elusive counterparts of γ-ray sources with respect to other extragalactic classes (Massaro et al. 2013a; D'Abrusco et al. 2013). All the above exhibits the importance of carrying out optical spectroscopic observations and hence the importance of following up our campaign.

In this paper we show the most recent results of the campaign. The sample was selected according to the criteria mentioned in Section 2. The sources were observed with OAN-

[16] https://heasarc.gsfc.nasa.gov/W3Browse/fermi/fermilpsc.html

SPM, SOAR, NTT, and Víctor Blanco telescope. We confirm the blazar nature of these sources and provide classification and redshift estimations. Finally, we summarize our results and provide a full overview of the sources that have been classified since the beginning of the campaign.

The paper is organized as follows. In Section 2 we briefly describe the method employed to select the sources analyzed in this work, while in Section 3 we outline the observations performed and the data reduction procedures. In Section 4 the results of the analyses performed are illustrated and, finally, Section 5 is devoted to our summary and conclusions. Unless otherwise stated, we adopt cgs units for numerical results and we also assume spectral indices, α defined by flux density $S_\nu \propto \nu^{-\alpha}$, and WISE magnitudes at [3.4], [4.6], [12], and [22] μm (i.e., the nominal WISE bands) are in the Vega system. We assume a flat cosmology with $H_0 = 72\,\mathrm{km\,s^{-1}\,Mpc^{-1}}$, $\Omega_M = 0.26$, and $\Omega_\Lambda = 0.74$ (Dunkley et al. 2009).

2. Sample Selection

During the optical campaign, we have selected our targets on the basis of the following criteria:

1. BCUs already assigned as counterparts to 4FGL catalog sources, but with no confirmation of their blazar nature.
2. Radio and X-ray sources located within the γ-ray positional uncertainty of UGSs (Marchesini et al. 2020).
3. BL Lacs with no optical spectrum available in the literature, or lacking a redshift estimate.
4. UGSs having a WISE source with blazar-like mid-IR colors lying within their positional uncertainty region, most of them being part of the WISE Blazar-like Radio-Loud Sources and Roma-BZCAT.

The sources that comprise our sample were selected according to points 1, 3, and 4. Additionally, we request small samples of sources in each observing proposal to make them more likely to be chosen.

A total of 39 sources were selected for this work: 37 are BCUs, one of them (4FGL J1259.5+2332, a.k.a. WISE J125949.83−322328.8) is claimed to be a BL Lac in the 4FGL, and a potential blazar-like counterpart of the UGS 4FGL J2114.9−3326 (a.k.a. WISE J211452.10−332533.8) was selected thanks to its mid-IR colors and lies within the position uncertainty region of the Fermi source. Additionally, we carried out an extensive literature check of these sources and we did not find optical spectra already available, except for 6 of the 39 sources, which we already observed and reported. During the campaign, we occasionally reobserve some sources to obtain their spectrum with a better signal-to-noise ratio and/or to detect them in a quiescent state in order to investigate if they are changing-look blazars and/or to measure their redshift.

The observing logbook of the selected sources is presented in Table 1.

3. Observations and Data Reduction

3.1. OAN-SPM

16 sources were observed with the 2.1 m telescope of the OAN in San Pedro Mártir, Mexico. The telescope carries a Boller and Chivens spectrograph with a 1024×1024 pixels E2V 4240 CCD, tuned to the 4000–8000 Å range, a dispersion of 2.26 Å pixel^{-1}, and a slit width of 2.″5. This configuration results in a spectral resolution of 10 Å. Wavelength calibration was done using CuHeNeAr comparison lamps.

3.2. SOAR

Ten sources were observed with the 4.1 m SOAR telescope located in Cerro Pachón, Chile. We used the single, long-slit mode of the Goodman High Through-put Spectrograph (Clemens et al. 2004) with a slit width of 1″ and a grating of 400l mm^{-1}, giving a dispersion of ∼3 Å pixel^{-1} in a spectral range from ∼4100 Å up to 7900 Å, and resolution of ∼6 Å. We used HgArNe lamps to perform wavelength calibration.

3.3. NTT

Nine sources were observed at the NTT. We performed long-slit spectroscopic observations using the EFOSC2 spectrograph with grism No. 13 and a slit width of 1″. This instrument configuration gave a spectral range of 3700–9000 Å and a dispersion of 2.77 Å pixel^{-1}. After each target, we observed HeAr comparison lamps to perform the wavelength calibration.

3.4. Blanco

Four sources were observed in remote mode at the Víctor Blanco 4 m telescope in Cerro Tololo, Chile. We made use of the COSMOS spectrograph, red grism (r2k), 1.″2 slit width at blue position, and the GG495 filter. This setup gave a spectral range of about 5000–9075 Å and a dispersion of 1 Å pixel^{-1}. We acquired HgAr comparison lamp spectra on each target position for the wavelength calibration.

3.5. Data Reduction Procedure

We carried out the data reduction using `IRAF` reduction packages (Tody 1986). First, for each acquisition we performed bias subtraction and flat-field correction. For the majority of the sources, we obtained three exposures which we combined using the median. To remove the cosmic rays left after the combination, we used the `imedit` task of `IRAF`. We performed wavelength calibration using comparison lamps taken for each object. Then, we subtracted background with the `background` task of `IRAF` and proceeded to extract the 1D spectrum with `apall` task. Finally, we performed flux calibration using standard stars observed during the same night; the flux calibration uncertainties in the spectra are ∼10%. The spectra were normalized to the continuum in order to make emission and absorption features more evident. The final spectra with their normalized version are shown in Appendix, along with the finding charts of each source.

We inspected each spectrum and searched for quasar-like emission lines from Lyα to Hα, based on the composite spectra of Vanden Berk et al. (2001). We also looked for host-galaxy absorption lines (Ca II H & K, *G* band, Balmer lines, Mg Ib, and Na I). Then, we fitted each line with a Gaussian profile and used the center wavelength for the redshift measurements. Additionally, we measured the EWs of all the emission/absorption lines.

4. Results

We successfully classified all the 39 sources in our sample and gave redshift estimates to 21 of them. We show the results in Table 2.

Table 1
Logbook of the Spectroscopic Observations of Our Sample

Fermi Name (1)	Fermi Class (2)	Fermi Association (3)	R.A. (J2000) (4)	Decl. (J2000) (5)	Telescope (6)	Date (yyyy/mm/dd) (7)	Exposure (s) (8)
4FGL J0002.4−5156	BCU	WISE J000229.20−515227.4	00:02:29.20	−51:52:27.5	SOAR	2021/09/13	3 × 900
4FGL J1008.0+0028	BCU	PKS 1005+007	10:08:11.44	+00:30:00.0	OAN-SPM	2021/05/11	3 × 1200
4FGL J1121.3−0011	BCU	MGC 0019706	11:21:19.43	−00:13:16.5	OAN-SPM	2021/05/10	3 × 1200
4FGL J1129.5+3034	BCU	87 GB 112657.9+305242	11:29:37.30	+30:36:34.5	OAN-SPM	2021/05/13	3 × 1800
4FGL J1131.1−0944	BCU	1RXS J113104.6−094353	11:31:05.26	−09:44:06.5	NTT	2021/06/08	3 × 520
4FGL J1153.6−2553	BCU	NVSS J115338−255412	11:53:38.46	−25:54:13.2	NTT	2021/06/09	3 × 520
4FGL J1202.9+5141	BCU	TXS 1200+519	12:03:07.13	+51:40:30.7	OAN-SPM	2021/05/07	3 × 1800
4FGL J1249.3−0545	BCU	GALEXASC J124919.46−054539.7	12:49:19.36	−05:45:39.7	NTT	2021/06/08	3 × 520
4FGL J1259.5+2332	BLL	LEDA 4075145	12:59:49.84	−32:23:28.9	OAN-SPM	2021/06/02	3 × 1800
4FGL J1319.5−0045	BCU	PKS B1317−005	13:19:38.77	−00:49:40.0	OAN-SPM	2021/05/07	3 × 1800
4FGL J1329.4−0530	BCU	HE 1326−0516	13:29:28.62	−05:31:35.8	OAN-SPM	2021/05/11	3 × 1200
4FGL J1331.7−0647	BCU	NVSS J133146−064632	13:31:46.84	−06:46:33.2	OAN-SPM	2021/05/09	3 × 1800
4FGL J1339.0−2400	BCU	PKS 1336−237	13:39:01.74	−24:01:14.0	NTT	2021/06/09	3 × 610
4FGL J1427.4−1823	BCU	NVSS J142726−182303	14:27:25.93	−18:23:03.8	NTT	2021/06/08	3 × 520
4FGL J1441.7+1836	BCU	NVSS J144143+183706	14:41:43.51	+18:37:10.7	OAN-SPM	2021/05/08	3 × 1800
4FGL J1514.6−2044	BCU	PMN J1514−2043	15:14:33.51	−20:44:26.2	NTT	2021/06/09	3 × 520
4FGL J1544.3−0649	BCU	NVSS J154419−064913	15:44:19.65	−06:49:15.4	OAN-SPM	2021/05/07	3 × 1800
4FGL J1554.4−1215	BCU	GALEXASC J155432.61−121325.7	15:54:32.59	−12:13:25.2	NTT	2021/06/09	3 × 520
4FGL J1612.2+2828	BCU	TXS 1610+285	16:12:17.62	+28:25:46.4	OAN-SPM	2021/05/10	3 × 1200
4FGL J1627.7+0251	BCU	CLASS J1627+0251	16:27:54.15	+02:51:09.8	OAN-SPM	2021/05/08	1 × 1800
4FGL J1638.0+0042	BCU	NVSS J163809+004223	16:38:08.85	+00:42:22.5	OAN-SPM	2021/05/13	4 × 1800
4FGL J1730.6+3805	BCU	NVSS J173044+380452	17:30:44.80	+38:04:55.0	OAN-SPM	2021/06/02	3 × 1800
4FGL J1806.2+6143	BCU	TXS 1805+616	18:06:19.93	+61:41:18.5	OAN-SPM	2021/06/01	4 × 1800
4FGL J1848.1−4230	BCU	PMN J1848−4230	18:48:06.18	−42:30:26.5	Blanco	2021/08/20	3 × 900
4FGL J1934.2+6002	BCU	GALEXASC J193419.64+600139.5	19:34:19.63	+60:01:39.6	OAN-SPM	2021/06/01	3 × 1800
4FGL J1942.5−5827	BCU	SUMSS J194224−582824	19:42:24.67	−58:28:24.4	SOAR	2021/09/06	3 × 800
4FGL J1944.9−2143	BCU	1RXS J194455.3−214318	19:44:55.17	−21:43:19.3	SOAR	2021/09/13	3 × 900
4FGL J2001.9−5737	BCU	1RXS J200205.7−573644	20:02:04.20	−57:36:45.5	Blanco	2021/08/21	3 × 1800
4FGL J2025.3−2231	BCU	NVSS J202515−223016	20:25:15.18	−22:30:18.4	NTT	2021/06/08	3 × 520
4FGL J2040.1−4621	BCU	2MASS J20400660−4620180	20:40:06.63	−46:20:18.2	SOAR	2021/09/13	3 × 900
4FGL J2045.1−2346	BCU	NVSS J204457−234643	20:44:57.73	−23:46:44.5	SOAR	2021/10/05	3 × 900
4FGL J2114.9−3326	UGS		21:14:52.10	−33:25:33.9	NTT	2021/06/09	3 × 520
4FGL J2115.6−4938	BCU	MRSS 235−024179	21:15:44.67	−49:39:07.0	SOAR	2021/09/16	3 × 900
4FGL J2143.0−5501	BCU	CTS 0561	21:41:44.21	−55:09:29.8	SOAR	2021/09/16	3 × 800
4FGL J2229.2−6911	BCU	PKS 2225−694	22:29:00.19	−69:10:30.3	Blanco	2021/08/20	3 × 1500
4FGL J2240.3−1246	BCU	1RXS J224014.7−124736	22:40:15.13	−12:47:38.9	SOAR	2021/09/06	3 × 800
4FGL J2309.7−3632	BCU	WISEA J230940.84−363248.7	23:09:40.84	−36:32:48.8	SOAR	2021/09/16	3 × 900
4FGL J2325.2−2010	BCU	NVSS J232520−201213	23:25:20.25	−20:12:12.8	SOAR	2021/09/06	3 × 900
4FGL J2348.1−4934	BCU	PKS 2346−498	23:49:25.38	−49:32:26.6	SOAR	2021/10/05	3 × 800

Note. In the Fermi association column we list the sources associated in the 4FGL.

We classified 19 out of the 39 sources in our sample as BZBs, 13 as BZGs, six as BZQs, and one as a normal elliptical galaxy (4FGL J1612.2+2828, a.k.a. WISE J161217.62 +282546.3). It is also worth noting that some BZGs could be normal radio galaxies instead of BZBs having the emission of their host galaxies that dominates their broadband spectral energy distribution (Peña-Herazo et al. 2021b).

The source 4FGL J1259.5+2332, which was previously listed in the 4FGL as BL Lac, appears in our observations as BZG probably due to an ongoing quiescent state during our observations. The potential blazar-like counterpart of the source 4FGL J2114.9−3326 was classified as BZB with unknown redshift.

Six out of the 39 sources analyzed here were already observed and reported in our campaign (also included in Table 2). In this manner, we were able to derive for the first time the redshift of 4FGL J1331.7−0647 (a.k.a. WISE J133146.84−064633.1), a BZB for which we did not obtain its redshift before since in our past observations its spectrum was featureless. Here, with our most recent observations we obtained $z = 0.168 \pm 0.001$. For the five other sources, both the classifications and redshift estimates are in agreement with previous results.

Only two out of the 19 BZBs possess redshift estimates, the 13 BZGs have reliable redshifts, and five out of six of the BZQs have reliable redshift estimates as well. For the remaining BZQ, 4FGL J2229.2−6911 (a.k.a. WISE J222900.18−691030.2), we tentatively assigned $z = 0.908$ since there is only one emission line in its spectrum, presumably Mg II λ2798 Å.

Altogether, the redshifts of the BZBs and BZGs are within the range 0.063–0.426, which is in agreement with the distribution of Roma-BZCAT.

Table 2
Summary of the Spectra Analyzed in this Paper

Fermi Name	WISE Name	Class	$E(B-V)$	z	Line ID	EW (Å)	λ_{obs} (Å)	Type
(1)	(2)	(3)	(4)	(5)	(6)	(7)	(8)	(9)
4FGL J0002.4−5156	J000229.20−515227.4	BZQ	0.0121	1.089 ± 0.002	C III]	28	3967	E
…	…	…	…	…	[Ne IV]	6	5058	E
…	…	…	…	…	Mg II	35	5851	E
4FGL J1008.0+0028[a]	J100811.44+002959.9	BZB	0.0294	0.099 ± 0.001	K	5	4320	A
…	…	…	…	…	H	4	4359	A
…	…	…	…	…	*G* band	3	4733	A
…	…	…	…	…	Mg I	9	5681	A
…	…	…	…	…	Na I	3	6473	A
…	…	…	…	…	Hα	3	7229	E
4FGL J1121.3−0011	J112119.43−001316.5	BZG	0.0334	0.100 ± 0.001	K	10	4325	A
…	…	…	…	…	H	8	4364	A
…	…	…	…	…	*G* band	7	4735	A
…	…	…	…	…	Hβ	3	5355	A
…	…	…	…	…	Mg I	8	5686	A
…	…	…	…	…	Fe I	2	5793	A
…	…	…	…	…	Na I	7	6479	A
4FGL J1129.5+3034[b]	J112937.30+303634.4	BZB	0.0183	…	…	…	…	…
4FGL J1131.1−0944	J113105.26−094406.5	BZB	0.0297	…	…	…	…	…
4FGL J1153.6−2553	J115338.46−255413.2	BZB	0.0547	…	…	…	…	…
4FGL J1202.9+5141	J120307.12+514030.6	BZG	0.0195	0.063 ± 0.001	K	10	4185	A
…	…	…	…	…	H	9	4219	A
…	…	…	…	…	*G* band	6	4578	A
…	…	…	…	…	Hβ	3	5171	A
…	…	…	…	…	Mg I	22	5500	A
…	…	…	…	…	Na I	6	6264	A
…	…	…	…	…	[N II]	2	7000	E
4FGL J1249.3−0545	J124919.36−054539.7	BZG	0.0238	0.278 ± 0.001	[O II]	4	4762	E
…	…	…	…	…	K	3	5024	A
…	…	…	…	…	H	2	5072	A
…	…	…	…	…	[O III]	3	6392	E
…	…	…	…	…	Hα	4	8389	E
…	…	…	…	…	[N II]	5	8423	E
4FGL J1259.5+2332	J125949.83−322328.8	BZG	0.0792	0.270 ± 0.0004	K	9	4995	A
…	…	…	…	…	H	7	5042	A
…	…	…	…	…	*G* band	5	5471	A
…	…	…	…	…	Mg I	6	6572	A
4FGL J1319.5−0045[b]	J131938.76−004939.9	BZQ	0.0217	0.891 ± 0.0002	Mg II	55	5291	E
…	…	…	…	…	[O II]	38	7049	E
4FGL J1329.4−0530[b]	J132928.62−053135.7	BZQ	0.0256	0.578 ± 0.001	Mg II	27	4414	E
…	…	…	…	…	[O III]	9	7908	E
4FGL J1331.7−0647[b]	J133146.84−064633.1	BZB	0.0320	0.168 ± 0.001	K	3	4596	A
…	…	…	…	…	H	2	4641	A
…	…	…	…	…	*G* band	2	5026	A
…	…	…	…	…	Hβ	1	5681	A
…	…	…	…	…	Mg I	4	6043	A
4FGL J1339.0−2400	J133901.74−240113.9	BZB	0.0678	…	…	…	…	…
4FGL J1427.4−1823	J142725.93−182303.7	BZB	0.0645	…	…	…	…	…
4FGL J1441.7+1836	J144143.50+183710.7	BZB	0.0307	…	…	…	…	…
4FGL J1514.6−2044	J151433.51−204426.2	BZB	0.1285	…	…	…	…	…
4FGL J1544.3−0649	J154419.65−064915.3	BZG	0.1350	0.172 ± 0.001	K	2	4612	A
…	…	…	…	…	H	2	4650	A
…	…	…	…	…	*G* band	2	5046	A
…	…	…	…	…	Hβ	2	5700	A
…	…	…	…	…	Mg I	4	6056	A
4FGL J1554.4−1215	J155432.58−121325.1	BZB	0.1874	…	…	…	…	…
4FGL J1612.2+2828[c]	J161217.62+282546.3	galaxy	0.0382	0.053 ± 0.0004	[O II]	18	3928	E
…	…	…	…	…	K	11	4144	A
…	…	…	…	…	H	9	4182	A
…	…	…	…	…	*G* band	7	4536	A
…	…	…	…	…	Mg I	11	5450	A
…	…	…	…	…	Na I	5	6209	A
4FGL J1627.7+0251	J162754.15+025109.7	BZB	0.0581	…	…	…	…	…

Table 2
(Continued)

Fermi Name	WISE Name	Class	$E(B-V)$	z	Line ID	EW (Å)	λ_{obs} (Å)	Type
(1)	(2)	(3)	(4)	(5)	(6)	(7)	(8)	(9)
4FGL J1638.0+0042	J163808.84+004222.5	BZB	0.0789	…	…	…	…	…
4FGL J1730.6+3805	J173044.79+380454.9	BZG	0.0332	0.161 ± 0.001	K	6	4571	A
…	…	…	…	…	H	4	4609	A
…	…	…	…	…	*G* band	3	4995	A
…	…	…	…	…	Hβ	3	5646	A
…	…	…	…	…	Mg I	7	6005	A
4FGL J1806.2+6143	J180619.93+614118.4	BZQ	0.0328	1.138 ± 0.004	C III]	174	4068	E
…	…	…	…	…	Mg II	97	5973	E
4FGL J1848.1−4230	J184806.17−423026.4	BZB	0.0665	…	…	…	…	…
4FGL J1934.2+6002	J193419.62+600139.5	BZB	0.0509	…	…	…	…	…
4FGL J1942.5−5827	J194224.67−582824.4	BZG	0.0568	0.349 ± 0.0004	K	2	5305	A
…	…	…	…	…	H	3	5354	A
…	…	…	…	…	*G* band	1	5811	A
4FGL J1944.9−2143	J194455.16−214319.2	BZG	0.0733	0.426 ± 0.001	K	2	5607	A
…	…	…	…	…	H	2	5656	A
…	…	…	…	…	*G* band	2	6145	A
4FGL J2001.9−5737	J200204.19−573645.4	BZB	0.0416	…	…	…	…	…
4FGL J2025.3−2231	J202515.17−223018.4	BZB	0.0523	…	…	…	…	…
4FGL J2040.1−4621	J204006.62−462018.2	BZG	0.0288	0.323 ± 0.001	K	2	5205	A
…	…	…	…	…	H	2	5251	A
…	…	…	…	…	*G* band	1	5692	A
4FGL J2045.1−2346	J204457.73−234644.4	BZB	0.0467	…	…	…	…	…
4FGL J2114.9−3326	J211452.10−332533.8	BZB	0.1050	…	…	…	…	…
4FGL J2115.6−4938	J211544.67−493907.0	BZG	0.0230	0.280 ± 0.001	[O II]	22	4769	E
…	…	…	…	…	K	12	5040	A
…	…	…	…	…	H	13	5078	A
…	…	…	…	…	*G* band	7	5506	A
…	…	…	…	…	[O III]	5	6405	E
4FGL J2143.0−5501	J214144.21−550929.8	BZQ	0.0274	1.909 ± 0.002	Si IV]	21	4072	E
…	…	…	…	…	C IV	201	4505	E
…	…	…	…	…	C III]	46	5533	E
4FGL J2229.2−6911	J222900.18−691030.2	BZQ	0.0276	0.908?	Mg II	37	5340	E
4FGL J2240.3−1246	J224015.12−124738.9	BZG	0.0512	0.188 ± 0.0002	K	4	4673	A
…	…	…	…	…	H	3	4715	A
…	…	…	…	…	*G* band	3	5118	A
…	…	…	…	…	Mg I	4	6150	A
…	…	…	…	…	Na I	3	7005	A
4FGL J2309.7−3632	J230940.84−363248.7	BZB	0.0123	…	…	…	…	…
4FGL J2325.2−2010	J232520.25−201212.7	BZG	0.0229	0.302 ± 0.001	[O II]	1	4855	E
…	…	…	…	…	K	2	5118	A
…	…	…	…	…	H	1	5167	A
…	…	…	…	…	*G* band	1	5612	A
…	…	…	…	…	[O III]	1	6525	E
4FGL J2348.1−4934	J234925.37−493226.5	BZG	0.0124	0.163 ± 0.0004	[O II]	2	4336	E
…	…	…	…	…	K	1	4577	A
…	…	…	…	…	H	2	4614	A
…	…	…	…	…	*G* band	1	5008	A
…	…	…	…	…	[O III]	1	5767	E
…	…	…	…	…	[O III]	2	5825	E
…	…	…	…	…	Mg I	1	6019	A

Notes. $E(B-V)$ obtained from NASA/IPAC Infrared Science Archive. A: Absorption line, E: Emission line. Question marks indicate that the redshift is uncertain. Sources previously observed in the campaign are marked with the following subindices according to the paper where they were reported.
[a] Peña-Herazo et al. (2021a).
[b] Peña-Herazo et al. (2019).
[c] de Menezes et al. (2020).

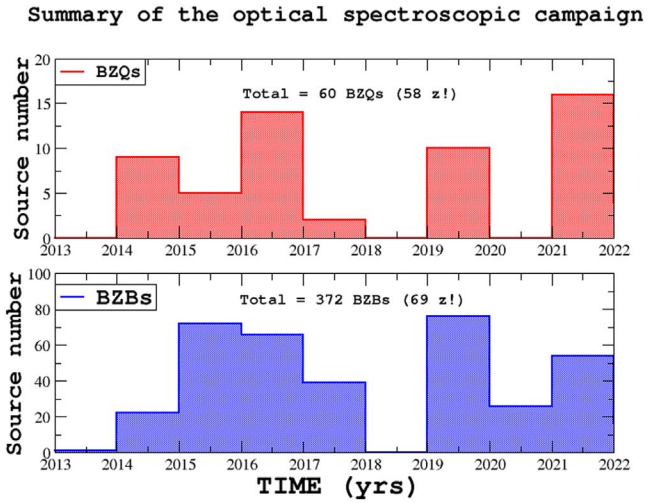

Figure 1. Summary of the number of sources classified per year thanks to our optical spectroscopic campaign. The upper panel shows the statistics of BZQs, while the lower panel shows the statistics of BZBs.

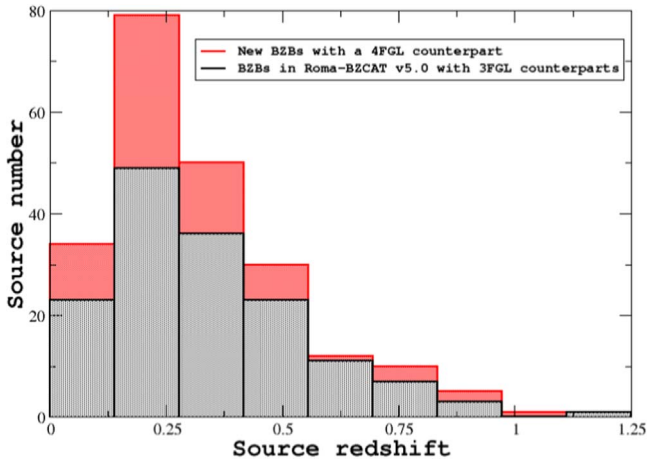

Figure 2. Comparison between the distribution of source redshifts for all BZBs listed in the Roma-BZCAT v5.0 with an assigned counterpart in the 3FGL (gray bars) and all BZBs discovered thanks to our optical spectroscopic campaign for which we were able to obtain a z measurement (red bars). Sources with uncertain redshifts are excluded.

5. Summary and Conclusions

In this paper we show the latest results of our optical spectroscopic campaign, which we started in 2013 aiming to identify/confirm the nature of Fermi-LAT sources classified as blazars of uncertain type and unidentified/unassociated sources. We observed a total of 39 sources with OAN-SPM, SOAR, NTT, and Víctor Blanco telescope.

1. In general, we classified 19 of them as BZBs, 13 as BZGs, six as BZQs, and one as a normal elliptical galaxy (4FGL J1612.2+2828).
2. The source 4FGL J1259.5+2332 was listed in the 4FGL as BL Lac, but in our observations its spectrum seems to be a BZG, most likely due to an ongoing quiescent state.
3. The source 4FGL J2114.9−3326 is listed in the 4FGL as UGS. We observed its potential low-energy counterpart, which was found on the basis of its mid-IR colors and lying within the uncertainty region of 4FGL J2114.9 −3326. The optical spectrum shows that it is a BZB with unknown redshift.
4. Six out of the 39 sources analyzed here were re-observed as a strategy to investigate if they are changing-look blazars and/or to measure redshifts. Both the classifications and redshift estimates are in agreement with our previous results, with the addition of the estimated redshift of $z = 0.168 \pm 0.001$ of the source 4FGL J1331.7 −0647, which was previously reported without redshift in the campaign.
5. We were able to provide reliable redshift estimates for 21 of the sources: two BZBs, all 13 BZGs, five BZQs, and for all sources identified and classified as elliptical galaxies. The redshift uncertainties are $\lesssim$1%.

We also point out that some BZGs could be normal radio galaxies instead of BZBs having the emission of their host galaxies that dominates their broadband spectral energy distribution (Peña-Herazo et al. 2021b).

Overall, thanks to our campaign we have classified 522 sources: 372 as BZBs, 60 as BZGs, 60 as BZQs, and 30 as normal elliptical galaxies. Figure 1 shows the statistics for BZBs and BZQs per year. For the BZBs, we provided reliable redshift estimates to 69 of them, while nine have upper or lower limits, 10 uncertain redshifts, and the remaining 285 do not possess redshift. For the BZGs, all of them have reliable redshift estimates; for the BZQs, 58 of them have reliable redshift estimates and two have uncertain redshift. The analysis of 323 of the total amount of BZBs, BZGs, and BZQs was performed with our observations; for the other 109 sources, the results were obtained with SDSS, LAMOST, and 6dFG archival searches. In contrast, during the period comprised by the campaign, we found 149 blazars in the literature: 143 BZBs, 2 BZGs, and 4 BZQs. From the 143 BZBs, 45 have reliable redshift, three are uncertain, 34 have upper or lower limits, and 61 have no redshift; the four BZQs and two BZGs have reliable redshifts.

In the beginning of the campaign, the amount of sources that we published per year went up to about 90 and then decreased toward 2018 mainly due to three factors: (i) we started pointing bright sources, thus our observing nights were very efficient in terms of number of targets observed, (ii) at that time we also submitted observation proposals at telescopes different from those available thanks to the Fermi-NOAO agreement as described in our publications, thus increasing the number of relatively bright sources classified, and (iii) at the beginning of our campaign we carried out the most extensive search in archives and databases as that of the Sloan Digital Sky Survey. In any case, during our optical spectroscopic campaign the number of classified/published targets follows that of awarded observing nights, considering a few months of delay for the data reduction, analysis, and publication.

In addition, we show in Figure 2 the comparison between (i) the distribution of source redshifts for all BZBs listed in the latest release of the Roma-BZCAT (i.e., v5.0) with an assigned counterpart in the 3FGL and (ii) all BZBs discovered thanks to our optical spectroscopic campaign, for which we were able to obtain a z measurement. Sources with uncertain redshifts (i.e., where only one line was identified and are shown with question marks in our publications and/or in the Roma-BZCAT) are excluded. We ran a Kolmogorov–Smirnov test and the null hypothesis that the two distributions are the same cannot be rejected. However, we can point out that most of the blazars for which we were able to estimate redshifts thanks to our spectroscopic campaign lie in the range 0.1–0.6.

Finally, it is worth noting that we will follow up our optical spectroscopic campaign, however, in the future we plan to reduce the number of papers but release more than 100 sources each.

We thank the anonymous referee for useful and valuable comments that led to improvements in the paper. This work was supported by CONACyT (Consejo Nacional de Ciencia y Tecnología) research grants 280789 and 320987 (Mexico). A. G.-P. and R.A.A.-A. acknowledge support from the CONACyT program for their PhD studies. V.C. acknowledges support from the Fulbright—García Robles scholarship. This work is supported by the MPIfR-Mexico Max Planck Partner Group led by V.M.P.-A. Based on observations obtained at the Southern Astrophysical Research (SOAR) telescope, which is a joint project of the Ministério da Ciência, Tecnologia, e Inovação (MCTI) da República Federativa do Brasil, the U.S. National Optical Astronomy Observatory (NOAO), the University of North Carolina at Chapel Hill (UNC), and Michigan State University (MSU). Based upon observations carried out at the Observatorio Astronómico Nacional on the Sierra San Pedro Mártir (OAN-SPM), Baja California, México. Part of this work is based on archival data, software or online services provided by the ASI Science Data Center. This publication makes use of data products from the Wide-field Infrared Survey Explorer, which is a joint project of the University of California, Los Angeles, and the Jet Propulsion Laboratory/ California Institute of Technology, funded by the National Aeronautics and Space Administration. We acknowledge TOPCAT[17] for the preparation and manipulation of the tabular data and the images.

Appendix
Optical Spectra and Finding Charts

In this Appendix we show the optical spectra (Figure 3) and the finding charts (Figure 4) of the 39 sources analyzed in this work. In Figure 3 the upper panels show the spectra with the identified lines (telluric lines are also indicated); the lower panels show the normalized spectra. The finding charts were retrieved from the 2nd Digitized Sky Survey (blue).

[17] http://www.star.bris.ac.uk/~mbt/topcat/

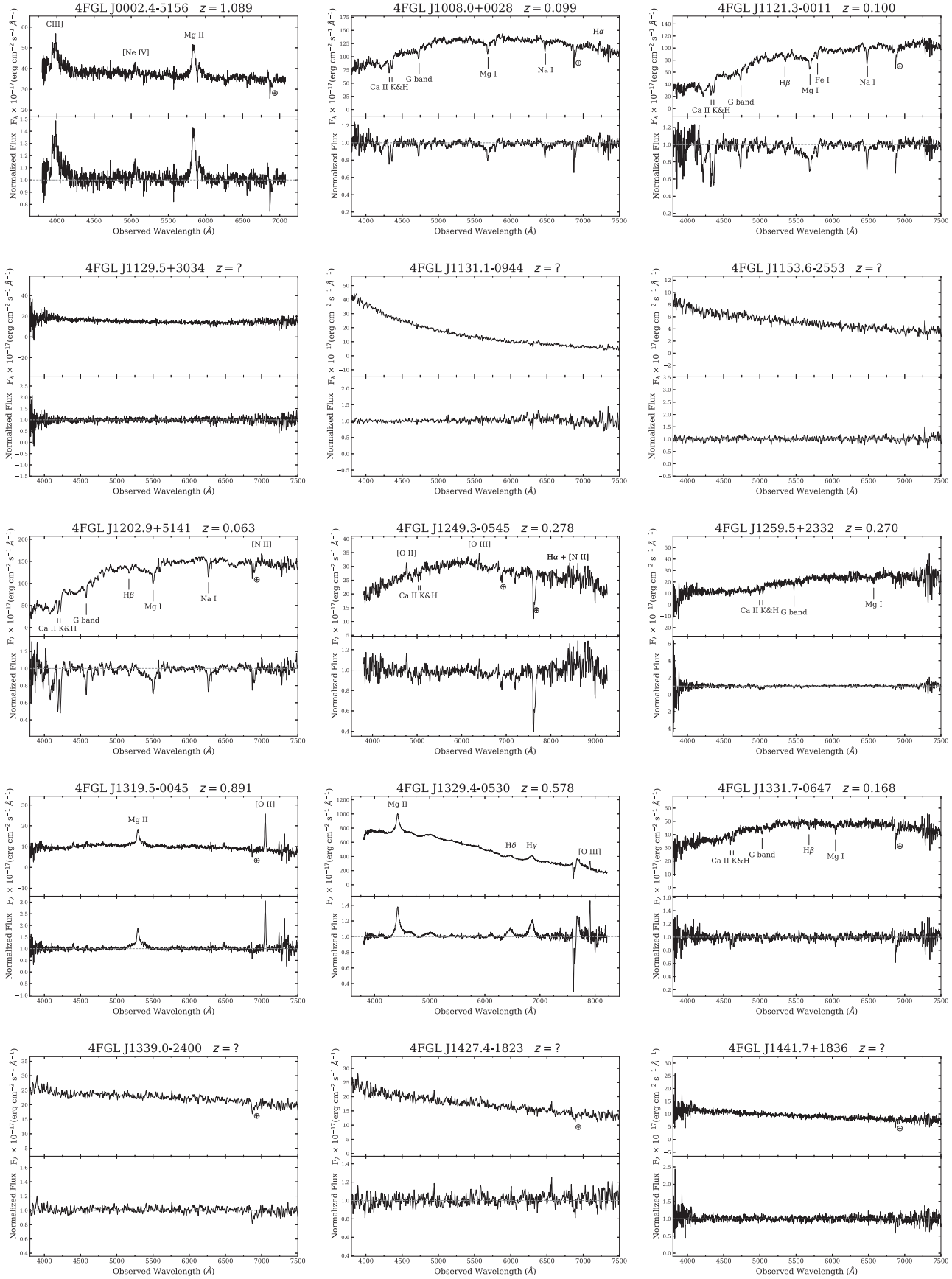

Figure 3. Optical spectra of the 39 sources analyzed in this work. (An extended version of this figure is available.)

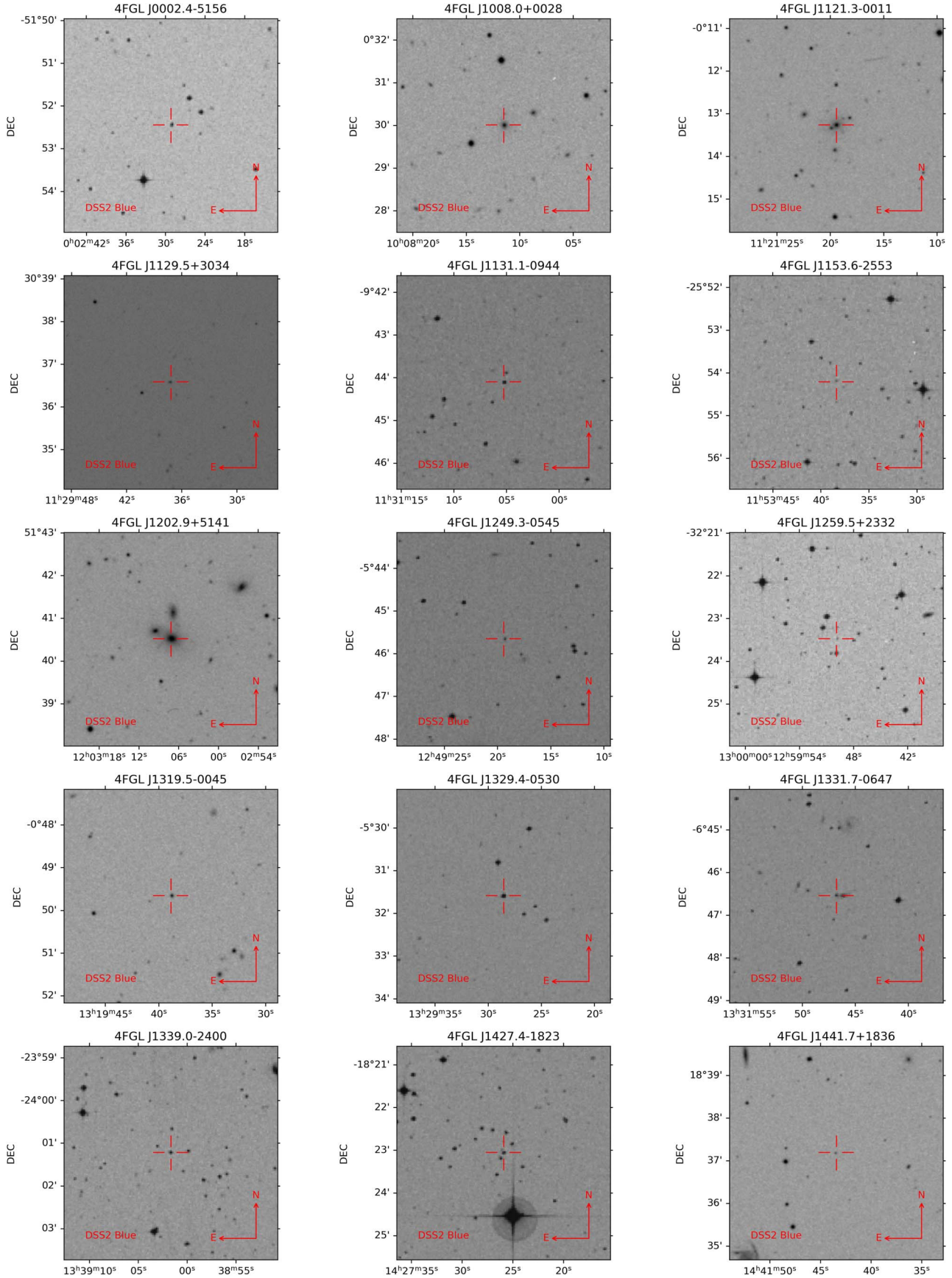

Figure 4. Finding charts of the 39 sources analyzed in this work, retrieved from the 2nd Digitized Sky Survey (blue). (An extended version of this figure is available.)

ORCID iDs

Abigail García-Pérez https://orcid.org/0000-0002-9896-6430
Harold A. Peña-Herazo https://orcid.org/0000-0003-0032-9538
Francesco Massaro https://orcid.org/0000-0002-1704-9850
Vahram Chavushyan https://orcid.org/0000-0002-2558-0967
Raffaele D'abrusco https://orcid.org/0000-0003-3073-0605
Nicola Masetti https://orcid.org/0000-0001-9487-7740
Marco Landoni https://orcid.org/0000-0003-2204-8112
Fabio La Franca https://orcid.org/0000-0002-1239-2721
Víctor M. Patiño-Álvarez https://orcid.org/0000-0002-5442-818X
Raúl A. Amaya-Almazán https://orcid.org/0000-0002-9443-7523
Dan Milisavljevic https://orcid.org/0000-0002-0763-3885
Alessandro Paggi https://orcid.org/0000-0002-5646-2410
Federica Ricci https://orcid.org/0000-0001-5742-5980

References

Abdo, A. A., Ackermann, M., Ajello, M., et al. 2010a, ApJ, 715, 429
Abdo, A. A., Ackermann, M., Ajello, M., et al. 2010b, ApJS, 188, 405
Abdollahi, S., Acero, F., Ackermann, M., et al. 2020, ApJS, 247, 33
Abdollahi, S., Acero, F., Baldini, L., et al. 2022, ApJS, 260, 53
Acero, F., Ackermann, M., Ajello, M., et al. 2015, ApJS, 218, 23
Acero, F., Ackermann, M., Ajello, M., et al. 2016, ApJS, 224, 8
Acero, F., Donato, D., Ojha, R., et al. 2013, ApJ, 779, 133
Ackermann, M., Ajello, M., Allafort, A., et al. 2011, ApJ, 743, 171
Ackermann, M., Ajello, M., Asano, K., et al. 2013, ApJS, 209, 11
Ajello, M., Angioni, R., Axelsson, M., et al. 2020, ApJ, 892, 105
Ajello, M., Arimoto, M., Axelsson, M., et al. 2019, ApJ, 878, 52
Ajello, M., Gasparrini, D., Sanchez-Conde, M., et al. 2015, ApJL, 800, L27
Ajello, M., Romani, R. W., Gasparrini, D., et al. 2014, ApJ, 780, 73
Álvarez Crespo, N., Masetti, N., Ricci, F., et al. 2016a, AJ, 151, 32
Álvarez Crespo, N., Massaro, F., Milisavljevic, D., et al. 2016b, AJ, 151, 95
Arsioli, B., Fraga, B., Giommi, P., Padovani, P., & Marrese, P. M. 2015, A&A, 579, A34
Atwood, W. B., Abdo, A. A., Ackermann, M., et al. 2009, ApJ, 697, 1071
Berlin, A., & Hooper, D. 2014, PhRvD, 89, 016014
Bernieri, E., Campana, R., Massaro, E., Paggi, A., & Tramacere, A. 2013, A&A, 551, L5
Campana, R., Massaro, E., & Bernieri, E. 2016, Ap&SS, 361, 183
Campana, R., Massaro, E., Bernieri, E., & DAmato, Q. 2015, Ap&SS, 360, 19
Clemens, J. C., Crain, J. A., & Anderson, R. 2004, Proc. SPIE, 5492, 331
Cutini, S., Lott, B., Gasparrini, D., et al. 2014, AAS Meeting Abstracts, 223, 115.08
D'Abrusco, R., Massaro, F., Ajello, M., et al. 2012, ApJ, 748, 68
D'Abrusco, R., Massaro, F., Paggi, A., et al. 2013, ApJS, 206, 12
de Menezes, R., Amaya-Almazan, R. A., Marchesini, E. J., et al. 2020, Ap&SS, 365, 12
Desai, A., Marchesi, S., Rajagopal, M., & Ajello, M. 2019, ApJS, 241, 5
Dunkley, J., Komatsu, E., Nolta, M. R., et al. 2009, ApJS, 180, 306
Ghisellini, G., Tavecchio, F., Foschini, L., & Ghirlanda, G. 2011, MNRAS, 414, 2674
Healey, S. E., Romani, R. W., Taylor, G. B., et al. 2007, ApJS, 171, 61
Hovatta, T., Lister, M. L., Aller, M. F., et al. 2012, AJ, 144, 105
Klindt, L., van Soelen, B., Meintjes, P. J., & Väisänen, P. 2017, MNRAS, 467, 2537
Landoni, M., Falomo, R., Treves, A., Scarpa, R., & Reverte Payá, D. 2015a, AJ, 150, 181
Landoni, M., Massaro, F., Paggi, A., et al. 2015b, AJ, 149, 163
Landt, H., Padovani, P., & Giommi, P. 2002, MNRAS, 336, 945
Marchesi, S., Kaur, A., & Ajello, M. 2018, AJ, 156, 212
Marchesini, E. J., Paggi, A., Massaro, F., et al. 2020, A&A, 638, A128
Marchesini, E. J., Pena-Herazo, H. A., Alvarez Crespo, N., et al. 2019, Ap&SS, 364, 5
Massaro, F., Alvarez Crespo, N., D'Abrusco, R., et al. 2016, Ap&SS, 361 337
Massaro, F., D'Abrusco, R., Ajello, M., Grindlay, J. E., & Smith, H. A. 2011, ApJL, 740, L48
Massaro, F., D'Abrusco, R., Giroletti, M., et al. 2013a, ApJS, 207, 4
Massaro, F., D'Abrusco, R., Tosti, G., et al. 2012, ApJ, 752, 61
Massaro, F., Landoni, M., D'Abrusco, R., et al. 2015, A&A, 575, A124
Massaro, F., Marchesini, E. J., D'Abrusco, R., et al. 2017, ApJ, 834, 113
Massaro, F., Paggi, A., Errando, M., et al. 2013b, ApJS, 207, 16
Nolan, P. L., Abdo, A. A., Ackermann, M., et al. 2012, ApJS, 199, 31
Paggi, A., Milisavljevic, D., Masetti, N., et al. 2014, AJ, 147, 112
Paiano, S., Falomo, R., Treves, A., Franceschini, A., & Scarpa, R. 2019, ApJ, 871, 162
Peña-Herazo, H. A., Marchesini, E. J., Alvarez Crespo, N., et al. 2017, Ap&SS, 362, 228
Pena-Herazo, H. A., Massaro, F., Chavushyan, V., et al. 2019, Ap&SS, 364, 85
Peña-Herazo, H. A., Massaro, F., Gu, M., et al. 2021b, AJ, 161, 196
Peña-Herazo, H. A., Paggi, A., García-Pérez, A., et al. 2021a, AJ, 162, 177
Ricci, F., Massaro, F., Landoni, M., et al. 2015, AJ, 149, 160
Stickel, M., Fried, J. W., & Kuehr, H. 1993, A&AS, 98, 393
Stickel, M., Fried, J. W., Kuehr, H., Padovani, P., & Urry, C. M. 1991, ApJ, 374, 431
Stocke, J. T., Morris, S. L., Gioia, I. M., et al. 1991, ApJS, 76, 813
Tody, D. 1986, Proc. SPIE, 627, 733
Urry, C. M., & Padovani, P. 1995, PASP, 107, 803
Vanden Berk, D. E., Richards, G. T., Bauer, A., et al. 2001, AJ, 122, 549
Wagner, S. J., & Witzel, A. 1995, ARA&A, 33, 163
Zechlin, H.-S., & Horns, D. 2012, JCAP, 2012, 050